

# A LARGE SELF-DEPLOYING STRUCTURE CONCEPT FOR SPACE TELESCOPE MISSIONS

R. Slade<sup>(1)</sup>, C. Brown<sup>(2)</sup>

<sup>(1)</sup>*Astrium Ltd, Gunnels Wood Road, Stevenage, Herts, UK, Email: richard.slade@astrium.eads.net*

<sup>(2)</sup>*Astrium Ltd, Gunnels Wood Road, Stevenage, Herts, UK, Email: craig.brown@astrium.eads.net*

## ABSTRACT

This paper describes a generic concept which permits stiff cylindrical structures with large polygonal cross-sections and lengths of tens of metres to be deployed by spacecraft in orbit. The concept utilises concertina folding geometry and tape-springs to enable the structure to self-deploy and latch from a compact stowed package. Potential x-ray and gamma-ray space telescope applications, exploiting the long focal length, high stiffness and dimensional stability of such structures are discussed. A low cost demonstrator model with 1 m x 1m cross-section has been built and deployment tested under 1 g conditions to prove the basic concept. High speed video recording has been used to correlate the dynamic behaviour with a simple analytical deployment model based on the measured stiffness characteristics of the tape-spring hinges.

## 1. INTRODUCTION

Orbiting telescope instruments working at short wavelengths (x-ray, gamma-ray) rely on grazing incidence or diffractive ‘optics’ to focus the incident photons onto the focal plane of the detectors. Because of the shallow angles of incidence necessary for high energy photons, it isn’t possible to use concave parabolic primary mirrors and folded optical paths to achieve a long focal length within a short tube in the same way as at visible and ultraviolet wavelengths. The focal length can only be achieved by physically separating the main focussing element and the detectors by this distance. As detection energies increase, the required focal length also increases. Long focal lengths of tens of metres are typically called for, requiring either formation-flying of multiple spacecraft elements or an extendable structure which can be packaged within the confines of the launch vehicle fairing and deployed in orbit to provide a stiff and stable ‘optical bench’. Synthetic aperture interferometer instruments also require large spatial separations to give the necessary resolving power and have even more exacting stability requirements.

To meet the requirements of these types of space telescope missions, Astrium Ltd are developing a generic self-deploying large tube structure concept based on concertina folding of rigid flat panels connected by tape-spring hinges which provide the

motive force for deployment and automatic latching (International Patent Application PCT / EP2010 / 058562). The deployed structures form closed cross-section beams with high bending and torsional stiffness. A wide range of configurations are possible, with different cross-sectional shapes and sizes varying from slender booms with diameters of a fraction of a metre to large extendable structures with cross-section dimensions similar to the main spacecraft body.

## 2. DEPLOYABLE STRUCTURE CONCEPT

The deployable structure concept consists of flat rigid panels which form the faces of a closed cross-section polygonal tube joined at their edges by tape-spring hinges. The tube length is made up of identical repeating bays of panels and hinges connected at frames, top and bottom, which provide shear continuity to the beam cross-section. By initiating buckling and elastic folding in the tape-spring hinges, the structure can be collapsed down to form a ‘flat-pack’ and restrained for launch. Release results in self-deployment by return of the elastic strain energy and self-latching due to the natural snap-out action of the tape-springs.

### 2.1. Structure Geometry

Some possible tube structure geometries are shown in Fig. 1. In principle the concept permits tubes with any regular or irregular faceted polygonal cross-section. The cross-section geometry can be optimised to provide the required configuration and structural performance within the stowage volume constraints. A larger number of sides increases the structural efficiency as the cross-section approaches the circular launch vehicle envelope, but the diminishing returns are offset by an increasing part count and complexity.

The panels can be folded ‘inwards’ or ‘outwards’ for stowage (Fig. 2). For inward folding, the panels are stowed inside the deployed cross-section of the tube. This arrangement provides a large unobstructed internal diameter for the converging beam of a large aperture telescope and an efficient structural section. For outward folding, the panels are stowed outside the tube cross-section. Such an arrangement is more suited to slender boom-like structures.

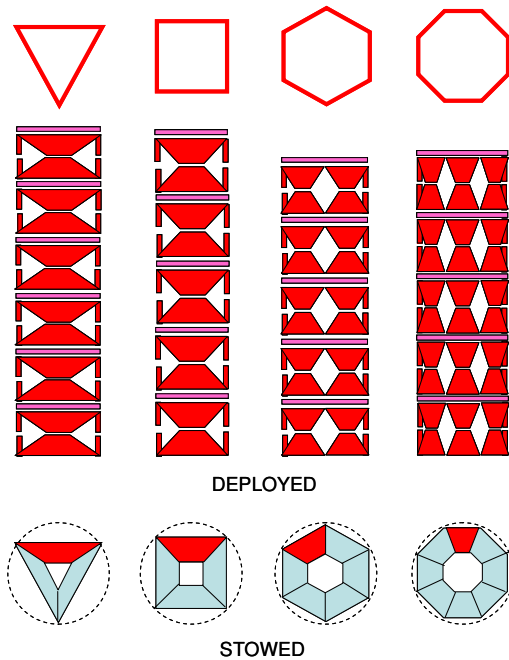


Figure 1. Some Deployable Structure Configurations.

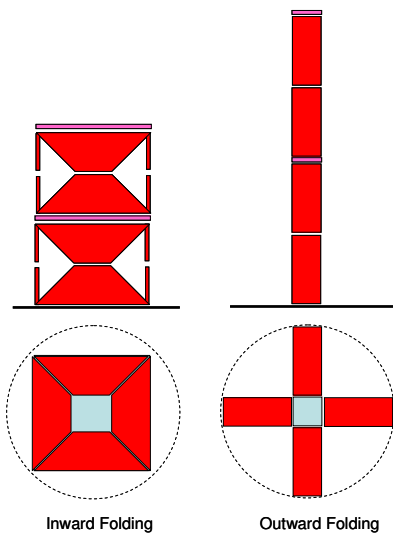


Figure 2. Stowage by Inwards and Outwards Folding

Kinematically, both modes of folding and deployment are the same (in one the folds are  $+180^\circ$  and in the other they are  $-180^\circ$ ) so the tape-spring hinges are conceptually identical, but it affects the panel geometry. Inwards folding constrains the panels to have a tapering shape so that they pack within internal area of the polygon. In the limit, to maximise packing efficiency, the panels could be triangular, tapering to a point. However, to provide sufficient edge length for mounting the tape-spring hinges and to preserve stiffness of the structural section, the panels have a trapezoidal shape. The packing factor (ratio of

deployed length to stowed height) is strongly affected by the choice of panel taper, i.e. the height of the trapeziums, since this defines the height of each bay when it is deployed. With outward folding it is not necessary to taper the panels. A higher packing factor can be achieved if the deployed tube cross-section is small, but the structural efficiency is considerably lower.

## 2.2. Tape-Spring Hinges

The hinges comprise linear arrays of tape-springs connecting the adjacent edges of the panels at the fold lines. The tape-springs are configured in a back-to-back configuration in which identical individual tape-springs are mounted in symmetric pairs either side of the panel thickness (Fig. 3).

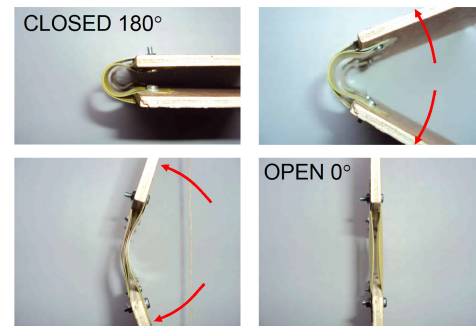


Figure 3. Back-to-Back Tape-Spring Hinge

When collapsed and elastically folded through  $180^\circ$  into the closed state for stowage, the outside tape-spring is subjected to equal sense bending (the fold curvature is in the same sense as the section transverse curvature) and the inside tape-spring is deformed into an 'S' shape, with opposite sense bending in the central part of its length, where it is constrained by the outer tape-spring, and equal sense bending at the ends. The stored elastic strain energy provides the motive hinge moment to open the folds and deploy the structure. At a critical opening angle (approx.  $25^\circ$ ) the bistable 'snap-out' characteristic of the tape-springs provides a self-latching function. The back-to-back arrangement results in a positive centring action when opening in either direction, minimising overshoot during deployment.

The tape-springs at the folds in the middle of each bay fold through  $180^\circ$ , but at the end frames these are divided into two and the tape-spring on each side of the frame folds through  $90^\circ$ . This arrangement permits each bay to be separately assembled and then bolted together at the frames to form the complete structure. A disadvantage is that the vertical leg length of the frame section for attachment of the tape-springs increases the stowed height and therefore reduces the packing factor that can be achieved. This can be avoided by attaching the frame at the mid-span of a single tape-spring hinge

folded through 180° using D-shaped clamps as shown in Fig. 4.

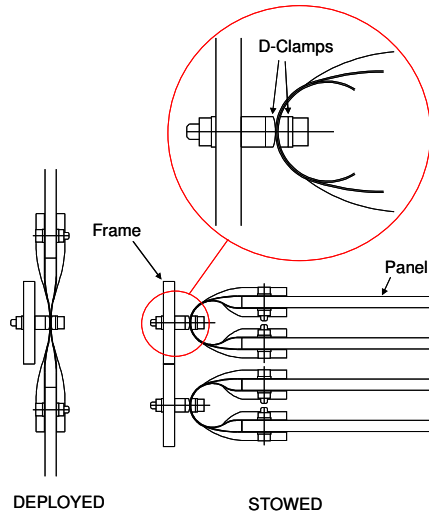


Figure 4. Frame Attachment to Tape-Spring Hinges

The minimum radius of curvature of the fold is controlled by selection of the unsupported tape-spring length and the thickness of the panels. A tight radius of curvature permits a closer separation of the stowed panels and improves the overall packing factor. However, the tightest acceptable radius curvature is constrained by the permitted strain limit of the material and the thickness necessary to provide the required hinge moments for deployment. Typically, the hinge moments must overcome resistances arising from the cold temperature flexure of electrical harness and thermal blankets. The achievable packing factor, and hence the maximum length of the structure that can be accommodated within the available stowage volume, is therefore related to the deployment resistances.

The hinge moment is provided by the aggregate effect of all the tape-springs along the panel edge at a given cross-section. To increase the moment where the edge length is constrained by the panel dimensions it is possible to 'nest' the tape-springs within each other to form multi-leaf springs which can still be folded to the radius of curvature of a single leaf tape-spring.

Spring steels provide the high failure strain and high Young's modulus required for tight radius of curvature folds and high hinge moments. However, in applications where low thermoelastic distortion or a low magnetic signature is required and where it is desirable to minimise mass, carbon-fibre reinforced composites can be employed in the tape-springs as well as the panels and frames. High strength PAN carbon fibres (e.g. T300, T800, T1000) are more attractive than higher modulus and pitch-based fibres because the higher failure strains offset the reduction in Young's modulus. Thermosetting resin systems (e.g. epoxies, cyanate esters) or thermoplastics (e.g.

polyetheretherketone = PEEK) are possible matrix materials. Thin plies are desirable to permit a tight deformed radius of curvature and allow lay-ups with multiple fibre angles for good shear as well as longitudinal and transverse structural properties. Woven materials offer high flexural strains to failure, although the apparent flexural modulus is also reduced in thin laminates due to fibre waviness within the fabric. Creep is also an issue in composite tape-springs, which must also be taken into consideration. Rows of composite tape-springs can be moulded as integral sets on a corrugated tool, with slots cut between the individual curved sections to permit flattening in the transverse direction when folded (Fig. 5). Integral flat flanges provide the bolted and / or bonded attachment interfaces to the panels, eliminating the need for curved spacers, which can add significant mass to the hinges.



Figure 5. Moulded Composite Tape-Spring Profile

### 2.3. Stowage and Deployment

The structure is assembled in the deployed configuration with the tape-spring hinges 'open' in the straight, unfolded condition. To stow a bay, the tape-spring hinges are collapsed by applying a lateral force inwards or outwards to form a fold in the desired direction. Once the hinge line is buckled, the bay is stowed down flat by applying an axial compressive force. The structure stack is restrained in the stowed configuration by compressive cup-cone contacts between the layers preloaded by a tensile hold-down system.

In the simplest deployment approach, the hold-down system is released and the structure self deploys as the elastic strain energy of the tape-springs is returned. As the tape-spring folds reach the critical snap-out angle the panels latch into the deployed position with minimum of overshoot and rebound. The speed of deployment can be fast and the latching shock relatively large, depending on the excess hinge moment motorisation over the resistances. It is possible to provide control over deployment speed by employing a rate-dependent damper, e.g. a rotary eddy current damper coupled to a spooled cable connecting the end frames of the structure. Alternatively, where a high degree of control or low shocks are required and structural stiffness is necessary during deployment, a canister type system could be used. In this deployment concept, the bays are individually released and opened from the top bay downwards and pushed out of a

stowage canister as the structure ‘grows’. In the simplest version of this arrangement the bay releases are sequentially triggered by an axially translating release mechanism. In a fully-controlled version, the opening of each bay is augmented / braked by an externally motorised axial translation mechanism.

### 3. POTENTIAL SPACE TELESCOPE APPLICATIONS

#### 3.1. X-Ray Observatory

A deployable tube structure to meet the requirements of the International X-Ray Observatory (IXO) mission has been studied. This application calls for an extendable optical bench structure to separate an instrument module from the  $\varnothing$  3.8 m grazing incidence main mirror assembly by a focal length of 20-25 m. The main mirror is supported at one end of a fixed structure which also houses the spacecraft systems externally around it. The length of the fixed structure is constrained by the long fairing of the Ariane 5 launcher, so the extendable part must deploy to a length of about 17 m (Fig. 6). The instrument module has a mass of 900 kg and the mass of the main spacecraft module including the main mirror is 4700 kg.

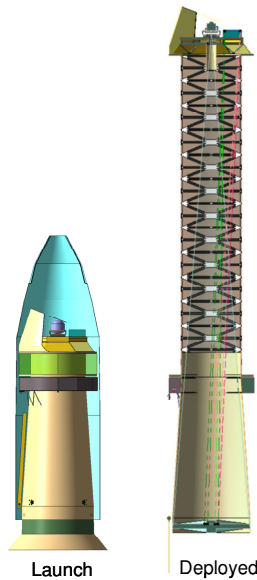


Figure 6. IXO Spacecraft Configuration

The deployable structure proposed has a square cross-section with a side length of 3 m made up of trapezium shaped panels which fold inwards for stowage within a  $\varnothing$ 4.3 m diameter circle. The panels have M55J carbon fibre / EX1515 cyanate ester composite skins bonded to an aluminium honeycomb core with a total thickness of 10 mm. The tape-spring hinges are back-to-back pairs with a modulus of 110 GPa, thickness of 0.25 mm, transverse radius of curvature of 18 mm and width of 25 mm.

Free-free normal modes analysis of the deployed structure has shown that the minimum frequency requirement of 1 Hz (specified to avoid coupling with the attitude control system) can be met with the main torsion and first bending modes predicted at 3.0 Hz and 3.1 Hz respectively (Fig. 7). A preliminary analysis indicated sufficient buckling stability in the locked-out tape-spring hinges to resist in-orbit manoeuvre loads without collapse. The estimated basic mass of the structure is 374 kg (22 kg/m or 1.83 kg/m<sup>2</sup>).

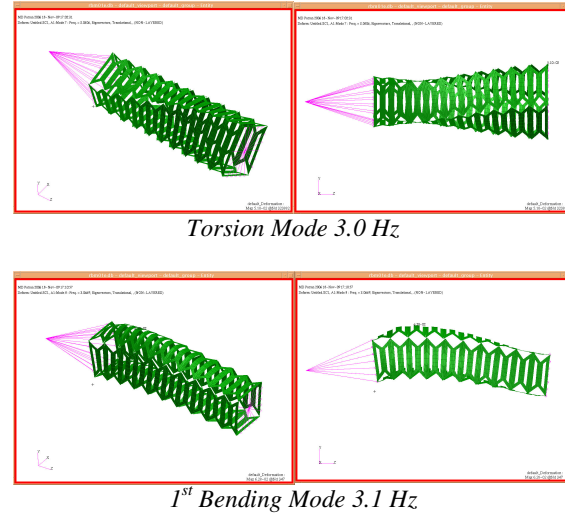


Figure 7. IXO Extendable Optical Bench Main Modes

#### 3.2. Gamma Ray Telescope

The concept has also been studied for a gamma-ray telescope which calls for a detector module to be separated from a  $\varnothing$ 1.2 m Laue lens mounted to the spacecraft bus with a focal length of 64 m. The detector and spacecraft bus modules have masses of 120 kg each. The spacecraft is to be accommodated within the fairing of the Taurus II launch vehicle. A relative lateral stability requirement of  $\pm$  0.1 m between detector and lens during 2 week observation periods and a minimum frequency requirement of 1 Hz were defined. The spacecraft is subjected to 0.001 rad/s<sup>2</sup> rotational accelerations during re-pointing slewing manoeuvres.

The proposed deployable structure has a hexagonal cross-section of  $\varnothing$ 3 m across the corners made up of trapezium shaped panels with a height of 0.8 m which fold inwards for stowage (Fig. 8). With a panel thickness of 10 mm and a minimum tape-spring fold radius of curvature of R15 mm it is possible to achieve a packing factor of 30, enabling the structure to be collapsed into a stowed height of less than 2.2 m, which can comfortably accommodate with the detector and spacecraft bus modules inside the launcher fairing.

Normal modes analysis predicted a 1<sup>st</sup> mode (bending) of 2.0 Hz when deployed to a length of 64 m. A large safety margin was found for tape-spring hinge buckling instability during slow manoeuvres. The thermoelastic pointing requirement is not particularly exacting and was considered to be achievable even with fairly large temperature gradients (reducing thermal blanketing needs). The estimated basic mass of the structure is 326 kg (5.1 kg/m or 0.57 kg/m<sup>2</sup>).

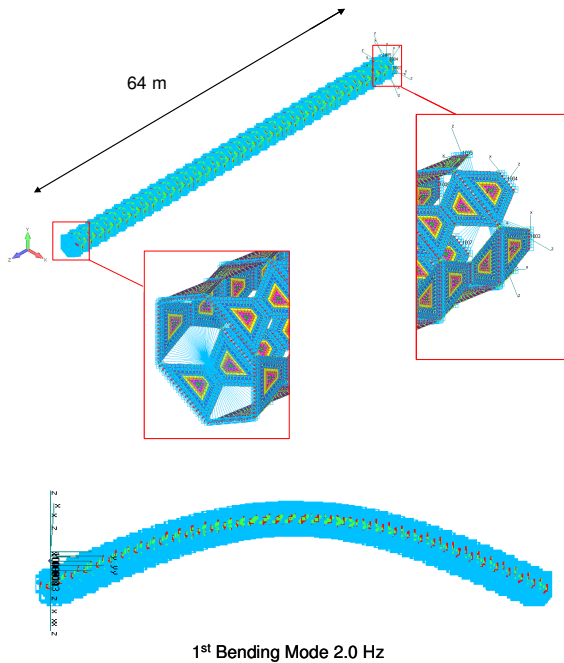


Figure 8. 64m Focal Length Gamma-Ray Telescope

### 3.3. Gamma Ray Instrument Boom

The deployable structure concept has also been studied for a lower cost gamma-ray mission with a similar Laue lens / detector configuration described above, but with a shorter focal length of 10 m. The support structure is essentially invisible in the gamma ray regime as gamma rays of this energy pass directly through it with no interaction. This allows the use of the more slender boom-like structure shown in Fig. 9. The cross-section is an equilateral triangle with a side length of 0.2 m. The panels have a narrow rectangular shape with a height of 1.0 m and fold outwards for stowage. The required focal length of 10 m can therefore be attained with only 5 bays and results in a low-profile stowed package.

Spacecraft bus and detector module masses are 360 kg and 120 kg respectively. Deployed normal mode frequencies of 0.67 Hz (torsion) and 3.6 Hz (1<sup>st</sup> bending) were predicted. Significant lightening cut-outs can be made in the panels whilst the minimum frequency requirement of 0.1 Hz for this spacecraft (to avoid attitude control system dynamic coupling) is still met.

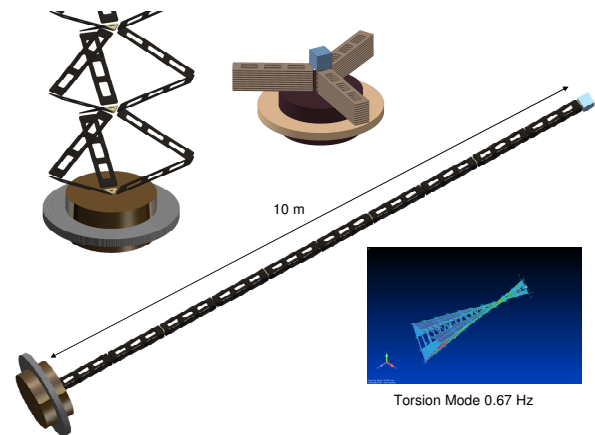


Figure 9. 10m Focal Length Gamma-Ray Instrument Boom

## 4. DEMONSTRATOR MODEL

### 4.1. Demonstrator Model Construction

To prove the basic concept, a low-cost deployment demonstrator model has been built (Fig. 10). This is a 1/3<sup>rd</sup> scale version of the IXO extendable optical bench square cross-section described above, but limited to a height of 4 bays (2 m). The trapezium-shaped panels are cut from marine plywood, the end frames are aluminium extrusions and the tape-spring hinges are cut from lengths of standard spring steel reel tape measures, attached with stainless steel M3 screws.

An objective of the model was to size it to be able to deploy in 1 g without the use of a gravity offload rig, permitting demonstrations anywhere which clearly show the deployment was self-motorised. For this reason it was necessary to grade the tape-spring hinge moments up the height of the structure, with higher moments at the hinges for the lower bays, which have to lift the weight of the bays above. These were sized by trial and error during manufacture. Consequently the tape-spring hinges are made up of single and double nested back to back pairs, and for the bays at the bottom of the stack, treble and quadruple pairs. It was also ultimately necessary to remove the uppermost bay to ensure deployment.

The model is deployed by a mechanical trigger which releases a pawl on a ratchet connected to the upper frame of the top bay via pulleys and cable restraint system. An adjustable friction brake can also be applied to tune the deployment speed. To stow the structure, special tools are used to collapse the tape-spring hinges on opposite faces one bay at a time. These are then winched down by the cables and



restrained by the pawl and ratchet. Safety pins guard against inadvertent release and deployment.

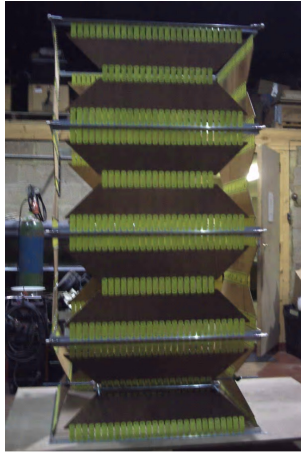


Figure 10. Demonstrator Model

#### 4.2. Tape Spring Hinge Characterisation

The hinge moment characteristics for single, double, triple and quadruple tape-spring pairs used in the demonstrator model were determined by simple static tests in which hinge moments necessary to achieve different equilibrium opening angles were found by suspending offset weights (Fig. 11). These show the typical relationship for an opening tape-spring hinge, with a decaying hinge moment from the fully closed angle ( $180^\circ$ ) to a critical angle of about  $20 - 25^\circ$  at which the snap-out behaviour results in a large increase in moment.

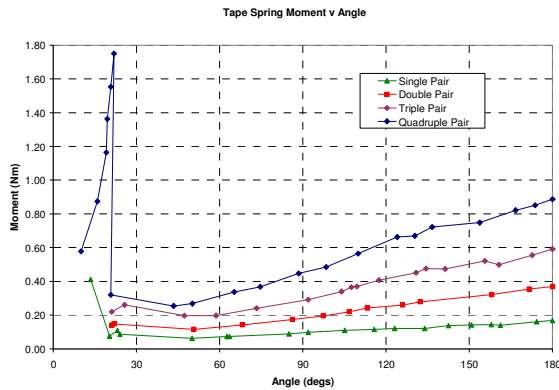


Figure 11. Tape Spring Hinge Moment vs Angle

These results showed that the moments from nested tape-springs were higher than would be estimated by linearly scaling on the basis of the number of tape-spring pairs. This suggests friction between the multiple leaves increases the effective bending section thickness.

#### 4.3. Deployment Tests

A series of deployment tests have been performed using the demonstrator model, recorded by high speed (slow motion) video and then analysed frame by frame. In addition to complete deployment tests of all 3 bays, further tests covered the release & deployment of just one or two bays at the top of the stack, or at the bottom with the bays above pre-deployed to provide a comprehensive dataset for subsequent analytical model correlation.

The deployments were filmed at 1000 frames/s (fps) with a shutter speed of  $1/3000$  s capturing square format images of  $1024 \times 1024$  pixels. In addition to the (upper frame) vertical positions of each bay, the panel opening angles were estimated from geometry. Video frames and the plotted vertical positions and panel angles for a full 3-bay deployment are shown in Figs. 12 & 13. Bays are numbered 1 to 3 from bottom to top. Fig. 14 is a close-up sequence of images showing the opening of a single bay.

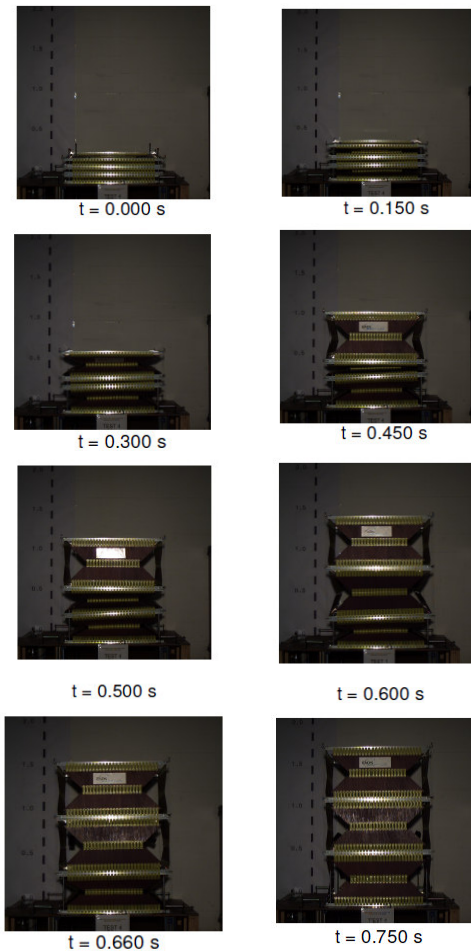


Figure 12. Demonstrator Model 3-Bay Deployment Test High Speed Video Images

The 3-bay deployment tests show that although the lowest bay (Bay 1) is the first to open, it is overtaken by the top bay (Bay 3) and then the middle bay (Bay 2), with it actually closing up slightly as the top bay latches out. Overall time to deploy is 0.75 s. The bay opening sequence can be partly explained by the uneven tape-spring hinge moments between the bays and the unequal resistance moments due to gravity.

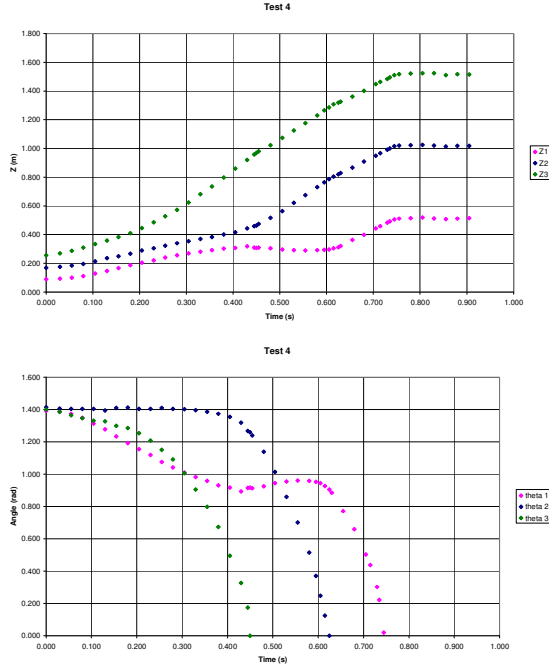


Figure 13. Demonstration Model Deployment Test Bay Positions and Panel Angles

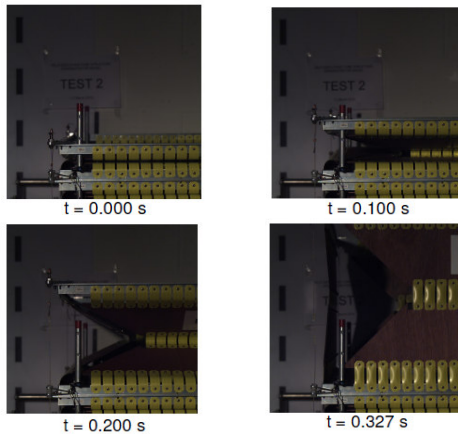


Figure 14. Demonstration Model Single Bay Deployment Test High Speed Video Images

#### 4.4. Deployment Shock Tests

Accelerometers were mounted to the demonstration model structure to record axial and lateral accelerations on the end frames during deployment. Enveloping Shock Response Spectra (SRS) computed from the data

are shown in Fig. 15. Highest shocks occur in the lateral direction because this is the velocity component of the tape-springs as they snap-out. The peak SRS level was 640 g at 1000 Hz.

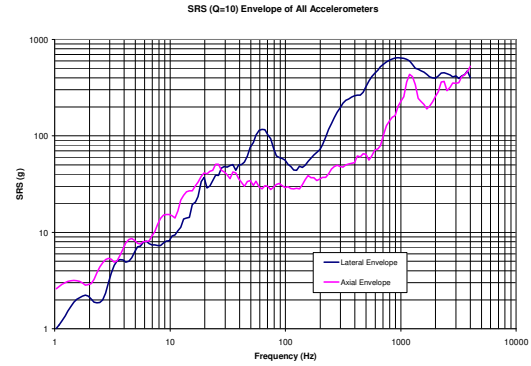


Figure 15. Demonstration Model Deployment Shock Response Spectra

## 5. DEPLOYMENT SIMULATION

### 5.1. Simulation Model Idealisation

A numerical model has been developed to simulate deployment dynamics in which the structure is idealised as shown in Fig. 16. Lagrange's equations (Eq. 1) were used to derive the coupled equations of motion for an N-bay structure (Eq. 3) by taking the panel angles,  $\theta_k$  ( $k = 1$  to  $N$ ) as the generalised coordinates.

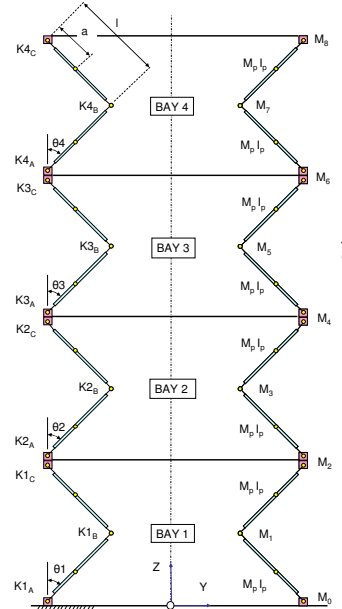


Figure 16. Numerical Deployment Model Idealisation

Lagrange's equations can be written as:

$$\frac{\partial}{\partial t} \left( \frac{\partial L}{\partial \dot{\theta}_k} \right) - \frac{\partial L}{\partial \theta_k} = Q_k \quad (1)$$

$L$  is the Lagrangian and  $Q_k$  are the generalised moments due to non-conservative forces.

$$L = T - U - S \quad (2)$$

$T$  = kinetic energy,  $U$  = potential energy (gravitational for 1 g deployment) and  $S$  = tape-spring strain energy.

The set of  $N$  equations of motion derived from (Eq. 1) in matrix format are:

$$[M]\{\ddot{\theta}_k\} + [C]\{\dot{\theta}_k^2\} + [D]\{\dot{\theta}_k\} + \{F_K\} = \{F_G\} + \{F_F\} \quad (3)$$

$[M]$  represents the generalised rotational inertia matrix,  $[C]$  represents the matrix of generalised centripetal moment coefficients,  $[D]$  is a generalised rate-dependent damping matrix,  $\{F_K\}$  are the generalised tape-spring hinge moments,  $\{F_G\}$  is a vector of generalised gravity hinge moments and  $\{F_F\}$  is a vector of generalised constant friction moments. The terms in these matrices and vectors are dependant on the angular positions  $\theta_k$ .

The simple bi-linear models shown in Fig. 17 were adopted for the tape-spring moments  $\{F_K\}$  using straight line fits to the measured characterisation data, based on the nesting configuration and number of tape-spring pairs along the hinge line. The snap-out latching action was idealised by an instantaneous jump to the unloading buckling moment at a critical angle (taken as 25°).

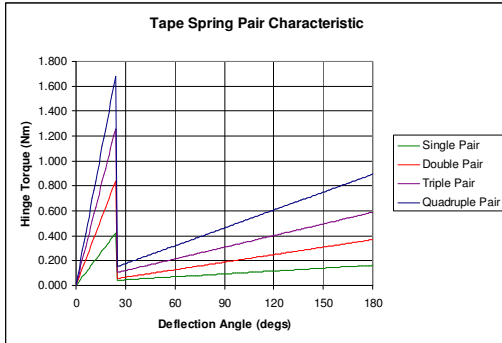


Figure 17. Tape Spring Hinge Model Idealisation

The equations of motion were solved using an Euler integration scheme from the specified initial conditions using a VisualBasic macro in Microsoft XL.

## 5.2. Numerical Simulations vs Test Data

The physical demonstrator model deployment tests described above were simulated using the numerical model. Fig. 18 compares the simulated panel angle time histories with test data for a 3-bay deployment test. The simulation agrees with the observed behaviour in terms of the bay opening sequence (including the overtaking effect) and general shapes of

the time histories but under-predicts the time of the first bay to deploy and slightly over-predicts the last. These differences are attributed to the over-simplified bi-linear tape-spring hinge model, particularly approaching the snap-out point, and rig effects such as friction, aerodynamic effects and pulley system inertia which were difficult to accurately quantify from the tests.

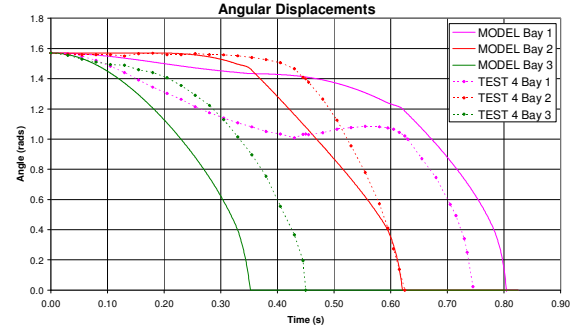


Figure 18. Demonstration Model Deployment Analysis vs Test Results

## 6. CONCLUSIONS

The basic concept of a deployable polygonal cross-section tube structure based on concertina folding of rigid panels with tape-spring hinges has been successfully demonstrated by deployment tests performed on a scale model. Studies have shown that this concept could be applied to large aperture telescope instruments requiring focal lengths in excess of 50 metres or as the supporting boom for smaller instruments requiring a component separation that cannot otherwise be accommodated in the launch vehicle. Technical complexities associated with formation flying (e.g. spacecraft attitude control and stray light problems) currently make formation flying for high energy astrophysics missions an unfavourable option. The Astrium Ltd deployable structure concept is therefore a potential mission enabling technology which offers a lower cost and lower risk alternative to formation-flying for large orbiting telescopes. A high packing efficiency allows long focal length x-ray and gamma-ray instruments to be accommodated within smaller, lower-cost launch vehicles, making such missions feasible. Its adaptability to a range of cross-sections and dimensions means it could also find applications in other deployable appendages, such as antennas, solar sail supports, magnetometers etc.

## 7. ACKNOWLEDGEMENTS

The authors would like to acknowledge Lee and Andy Fleming of LLF Solutions who built the Demonstrator Model and to apologise to DIY enthusiasts for the scarcity of reel tape measures in the surrounding locality during its construction. Thanks also to Andy Kiley, Ian Rathband & Abigail Hutty for the FE analysis and Mark Bonnar for CAD modelling.